



# A review of $T_s$ /VI remote sensing based methods for the retrieval of land surface energy fluxes and soil surface moisture

G. Petropoulos,<sup>1,3\*</sup> T.N. Carlson,<sup>2</sup> M.J. Wooster<sup>3</sup>  
and S. Islam<sup>4</sup>

<sup>1</sup>Department of Earth Sciences, University of Bristol,  
Wills Memorial Building, Queens Road, Bristol BS8 1RJ, UK

<sup>2</sup>Department of Meteorology, Pennsylvania State University,  
University Park, PA 16802, USA

<sup>3</sup>King's College London, Department of Geography, London WC2R 2LS, UK

<sup>4</sup>Department of Civil and Environmental Engineering, Tufts University,  
113 Anderson Hall, Medford, MA 02155, USA

**Abstract:** Imagery from remote sensing systems, often combined with ancillary ground information, is able to provide repetitive, synoptic views of key parameters characterizing land surface interactions, including surface energy fluxes and surface soil moisture. Differing methodologies using a wide range of remote sensing data have been developed for this purpose. Approaches vary from purely empirical to more complex ones, including residual methods and those that have their basis in the biophysical properties characterizing a two-dimensional  $T_s$ /VI (surface temperature/vegetation index) scatterplot domain derived from remote sensing observations. The present article aims to offer a comprehensive and systematic review of this latter group of methods, which differ in terms of the complexity and assumptions they entail as well as their requirement for field-based and other ancillary data. Prior to the review, the biophysical meanings and properties encapsulated in the  $T_s$ /VI feature space is elucidated, since these represent the building block upon which all the  $T_s$ /VI methods described herein are based. The overview of the  $T_s$ /VI methods is also very timely, as one such method is being scheduled in the operational retrieval of surface soil moisture content by the National Polar-orbiting Operational Environmental Satellite System (NPOESS), in a series of satellite platforms due to be launched in the next 12 years starting from 2016.

**Key words:** latent heat flux, remote sensing, sensible heat flux, surface soil moisture,  $T_s$ /VI methods.

---

\*Author for correspondence. Email: [george.petropoulos@bristol.ac.uk](mailto:george.petropoulos@bristol.ac.uk)

## I Introduction

Knowledge of both latent (LE) and sensible (H) heat fluxes, as well as of soil water content, are of great importance to many environmental applications, including the monitoring of plant water requirements, plant growth and productivity, as well as for irrigation and cultivation management procedures (Kustas *et al.*, 2004; Dodds *et al.*, 2005; Consoli *et al.*, 2006). Such data are also of key significance in the numerical modelling and prediction of atmospheric and hydrological cycles, and to improving the accuracy of weather forecast models (Jacob *et al.*, 2002). Furthermore, quantitative information on these parameters on a regional scale is important for the monitoring of land degradation and desertification (Xu and Chen, 2005; McCabe and Wood, 2006), for the understanding of processes that control ecosystem carbon dioxide ( $\text{CO}_2$ ) exchange (Yepez *et al.*, 2003) and for elucidating the interactions between these parameters and other ecosystem processes (Wever *et al.*, 2002).

The deployment of ground instrumentation for the estimation of LE and H fluxes (eg, eddy covariance systems or lysimeters), and also for soil moisture measurement (eg, gravimetric sampling, neutron normalization, time domain reflectometry), offers certain advantages. Some of the most important include their ability to provide measurements at different atmospheric levels and soil depths, the ease of instrument portability and rapidity/frequency, and the relative maturity of certain of the measurement methods. However, over large areas, ground instruments are usually able to provide only localized estimates of the surface energy fluxes and soil moisture content, and their implementation is often expensive and time-consuming as well as labour-intensive and sometimes subject to instrument failure.

The advent of satellite-based remote sensing over the last few decades has led to a considerable amount of work in determining whether such systems can provide spatially

explicit information relating to fluxes of LE, H and soil-moisture content variations. The general circumstances that make such satellite remote sensing techniques attractive for the retrieval of these parameters include their ability to provide repetitive, synoptic views in a spatially contiguous fashion, without a disturbing influence on the area to be surveyed and without site accessibility issues (de Troch *et al.*, 1996; Engman and Schultz, 2000). As a result, several algorithms have been proposed for the estimation of these parameters utilizing information from different types of remote sensing, often in combination with ancillary surface and atmospheric observations. In particular, the combined use of satellite data from optical and thermal infrared radiometers has shown promise for the retrieval of both LE and H fluxes and soil surface moisture variations (the latter defined as the water contained at the first 5 cm of the soil depth) (Sandholt *et al.*, 2002; Stisen *et al.*, 2008). The exact methods applied vary from purely empirical to more physically based approaches, including residual methods based on the energy balance equation and methods based on the information derived from the 'scatterplot' relationships between satellite-derived vegetation index (VI) and surface radiant temperature ( $T_s$ ) measures. Overviews of the various methodologies have been provided relatively recently by, for example, Moran *et al.* (2004), Courault *et al.* (2005) and Verstraeten *et al.* (2008). Although such overview studies have included a reference to the  $T_s$ /VI group of methods, to our knowledge, a systematic review of these particular approaches, including reference to the foundations and assumptions on which they are based, has not yet been made available. This is despite their relative advantages, including their requirement for relatively few parameters measurable over large areas, their potentially enhanced ability to deal with surface heterogeneity and their potential to provide easier transformation between instantaneous and daytime averaged fluxes.

Such characteristics also provide the potential for operational application (Nishida *et al.*, 2003b; Jiang and Islam, 2003). The aim of the present article is twofold: on the one hand to provide a useful and informative review of the development of methods to estimate land surface energy fluxes and surface soil moisture from remote sensing methods that utilize measurements capable of populating the  $T_s$ /VI feature space, and on the other hand to provide an inclusive overview of the biophysical properties characterizing this  $T_s$ /VI domain in relation to the estimation of the turbulent energy fluxes and soil surface moisture content. Understanding of the biophysical properties encapsulated within the  $T_s$ /VI domain is regarded as fundamental, since this is the building block upon which all the ( $T_s$ /VI) methods discussed herein are based. A review of  $T_s$ /VI-based methods is rather timely, since one such scheme has been proposed for the operational retrieval of surface soil moisture variations using the National Polar-orbiting Operational Environmental Satellite System (NPOESS), a series of platforms due to be launched in the next 12 years starting from 2016.

## **II Theoretical basis and biophysical properties of the $T_s$ /VI relationships**

### *1 Progress in relating the $T_s$ /VI scatterplot with biophysical properties*

Since the early 1980s, a number of studies have documented the emergence of a triangular or trapezoidal shape when remotely sensed  $T_s$  and VI measures taken from heterogeneous areas are plotted in two-dimensional feature space – forming a  $T_s$ /VI scatterplot. The focus of many of these studies has been the analysis of biophysical properties encapsulated in the  $T_s$ /VI pixel envelope, and to make associations between these and the estimation of land surface energy fluxes and surface soil moisture. Carlson *et al.* (1981) were among the first to underline a potentially discernible relationship between LE fluxes, soil moisture content

and fractional vegetation cover ( $F_r$ ). Goward *et al.* (1985) suggested the potential of using the scatterplot-derived rate of change of  $T_s$  with vegetation amount to diagnose the surface resistance to moisture fluxes. Hope *et al.* (1986) used simulations from a canopy reflectance model to confirm that an increase in vegetation amount, as indicated by a satellite-derived VI measure, resulted in a decrease in the area-averaged minimum canopy resistance and to an increase in LE. Nemani and Running (1989) used AVHRR data to relate the slope of the  $T_s$ /VI relationship over a coniferous forest in the USA to the regional surface resistance, a key input for the estimation of regional LE flux. Carlson and Buffum (1989) studied the  $T_s$ /VI feature space properties using the one-dimensional Boundary Layer Model of Goward *et al.* (1985). The authors discovered that changes in surface soil moisture could be described within the  $T_s$ /VI ‘triangular’ envelope as isopleths of surface soil moisture content plotted as a function of  $T_s$  and  $F_r$ , the latter parameter being calculated from the widespread Normalized Difference Vegetation Index (NDVI).

Carlson *et al.* (1990; 1995b) showed that the sensitivity of  $T_s$  to soil moisture variations differs for the leaf and surface soil around the plants, and tends to be much greater between areas of bare soil rather than across the leaves. This finding was very important since it confirmed their assumption that the triangular shape of the  $T_s$ /VI scatterplot emerges as a result of the much smaller sensitivity of  $T_s$  to surface soil water content over vegetated areas than over areas of bare soil. Ridd (1995), Carlson *et al.* (1995b) and Gillies and Carlson (1995) further illustrated how different parts of the  $T_s$ /VI triangle/trapezoidal space correspond to different biophysical properties, while Moran *et al.* (1994; 1996), Carlson *et al.* (1995b) and Gillies *et al.* (1995; 1997) used different spatial data sets to demonstrate that the boundaries of the triangular shape might be used to infer the physical constraints for the

solution of the surface energy fluxes and surface soil moisture availability  $M_o$  (Figure 1). Carlson *et al.* (1995a), using both high spatial resolution data from the airborne NS001 sensor (12.2 m) and also much coarser spatial resolution (1 km) satellite data from the NOAA Advanced Very High Resolution Radiometer (AVHRR), demonstrated that the apex of the  $T_s/VI$  scatterplot can be used to derive the screen-level air temperature ( $T_{air}$ ) with an accuracy of around 1°C. Carlson *et al.* (1995a) and Prihodko and Goward (1997) further suggested that the  $T_s/NDVI$  relationship could be used for the retrieval of  $T_{air}$ , based on the assumption that a fully vegetated canopy is in thermal equilibrium

with the local atmosphere due to the similar heat capacity of dense vegetation and air (Goward *et al.*, 1985). In parallel with these developments, Goetz (1997) and Goward *et al.* (2002) emphasized the value of analysing the  $T_s/NDVI$  scatterplot when making assessments of area-averaged soil moisture, while Symanzik *et al.* (2000) applied data mining techniques to explore the properties and transformations occurring in AVHRR data analysed in the  $T_s/VI$  domain as a function of season and land-cover type.

Sun *et al.* (2005) then used the crop water stress index (CWSI) and an aerodynamic resistance parameter derived from the  $T_s/NDVI$  scatterplot properties to propose

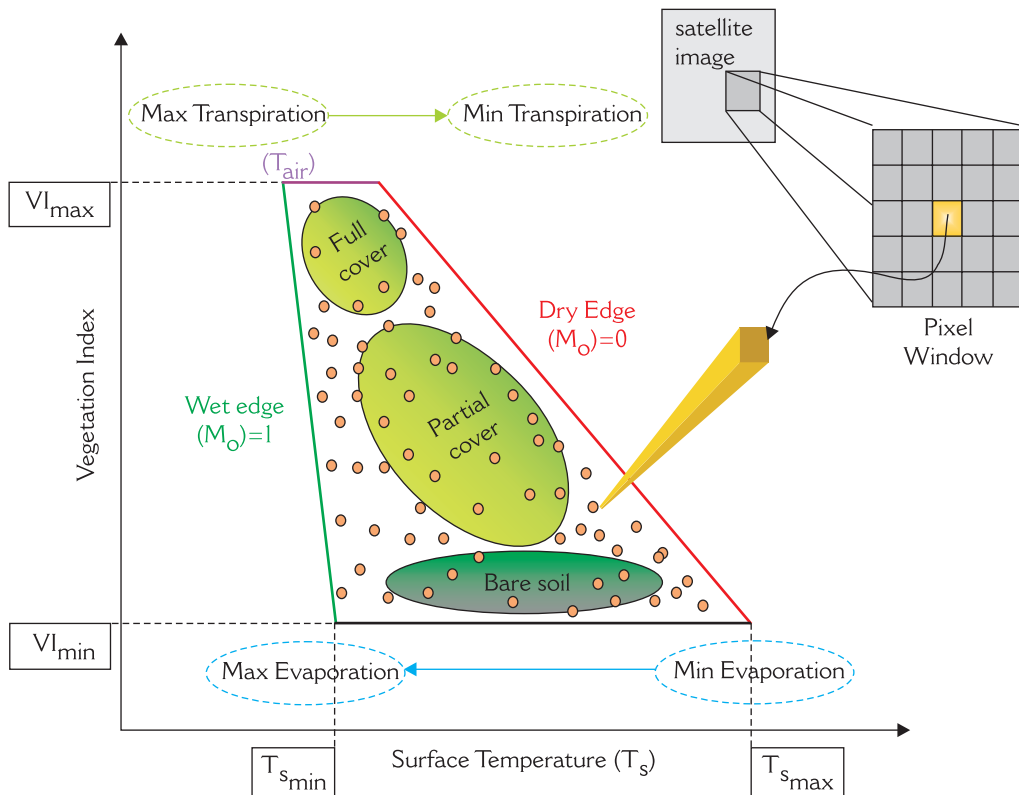


**Figure 1** Summary of the key descriptors and physical interpretations of the  $T_s/VI$  feature space or ‘scatterplot’

Source: Synthesized from previous works of Lambin and Ehrlich (1996), Sandholt *et al.* (2002) and Nishida *et al.* (2003a; 2003b).

a thermodynamic method for retrieving  $T_{\text{air}}$ , and, recently, Stisen *et al.* (2007) were able to map  $T_{\text{air}}$  to a root mean squared difference (RMSD) of better than 3°C compared to ground measurements over large areas of West Africa, based on contextual interpretations geostationary Meteosat SEVIRI observations made within the  $T_s$ /VI domain.

### *2 Interpretation of the physical properties encapsulated in $T_s$ /VI feature space*

Assuming that cloud-contaminated pixels and those containing standing water have been masked out from remotely sensed imagery, a series of per pixel values of  $T_s$  and VI collected from a satellite or airborne based radiometer over heterogeneous terrain usually form a triangular (or trapezoidal) shape in  $T_s$ /VI feature space as shown in Figure 1. In this representation, each small filled circle represents the measurements from a single pixel. Figure 1 also includes the main properties believed to be represented by the  $T_s$ /VI pixel envelope.

The emergence of the triangular (or trapezoid) shape in the  $T_s$ /VI feature space is the result of the low sensitivity of  $T_s$  to soil moisture variations over vegetated areas, but its increased sensitivity (and thus greater spatial variation) over areas of bare soil. Referring back to Figure 1, the right-hand border of the triangle (or trapezoid) (the so-called 'dry edge or warm edge') is defined by the locus of points of highest temperature but which contain differing amounts of bare soil and vegetation, and is assumed to represent conditions of limited surface soil moisture (Gillies and Temesgen, 2000). Likewise, the left-hand edge (the so-called 'wet edge or cold edge') corresponds to the set of cooler pixels that have varying amounts of vegetation cover and have the maximum soil water content. Variation along the lower edge (ie, the 'base') of the triangle (or trapezoid), is assumed to reflect the combined effects of soil water content and topography variations across areas of bare soil,

while the triangle's (or trapezoid's) apex equates to the status of full vegetation cover (expressed by the highest VI value). The remaining points within the triangular space correspond to pixels with varying vegetation cover, somewhere between bare soil and dense vegetation. For data points having the same VI,  $T_s$  can range markedly. When well supplied with water, transpiration acts to cool vegetation very effectively, but as vegetation undergoes water stress the plant tends to close its stomata – with the resulting transpiration decrease leading to an increase in leaf temperature. Thus, for pixels with the same VI, those with minimum  $T_s$  represent the case of the strongest evaporative cooling, while those with maximum  $T_s$  represent those with the weakest evaporative cooling. In this way, the triangle's (or trapezoid's) 'dry edge' is considered to represent the upper limit of evaporation for the different vegetation conditions found within the scene, whereas the reverse is implied for the 'cold edge'. The presence of a trapezoidal rather than perfectly triangular  $T_s$ /VI feature space plot is produced by  $T_s$  increasing when the VI remains at the maximum value, and is interpreted to result from variations in soil thermal inertia with changing soil water content (which affects the soil heat storage and therefore the soil temperature) (Carlson, 2007; Murray and Verhoef, 2007). The relatively narrow vertex of the triangular envelope (Figure 1) expresses the comparatively low sensitivity of leaf temperature to changes in soil water content when compared to bare soil, the much greater sensitivity of which is evidenced by the triangle's much wider base.

### *3 Factors influencing formation of the $T_s$ /VI envelope*

A number of studies have been concerned with examining the main factors driving the shape of the  $T_s$ /VI scatterplot that has been elucidated in the previous section. Smith and Choudhury (1991) studied the changing slope of the  $T_s$ /NDVI relationship in a variety of land-cover types, concluding that some of

the most influential parameters were evaporation from the soil and the leaf stomatal resistance. Nemani *et al.* (1993) found the  $T_s$ /NDVI slope to be primarily controlled by vegetation fractional cover, surface moisture status and local meteorology. Carlson *et al.* (1995b) resampled airborne remote sensing data to four different spatial resolutions (5, 20, 80 and 320 m) and demonstrated that the triangular shape in the  $T_s$ /VI domain is more dependent on the number of pixels in the scene than on the spatial resolution of the measurements. The implication was that the triangular/trapezoidal concept had the potential to be extended to regional scales and operational uses through the exploitation of remote sensing satellites. Goward *et al.* (2002) employed a simple biosphere model, parameterized using data from the HAPEX-Mobilhy field experiment (André *et al.*, 1986), and examined the sensitivity of the  $T_s$ /VI relationship to a series of biophysical and atmospheric parameters. Their results, although somewhat site-specific, indicated the highly influential effect of surface soil moisture and incident radiation variations on the specific position of pixels within the  $T_s$ /VI feature space. Lambin and Ehrlich (1996) and Sandholt *et al.* (2002) later summarized the most important biophysical determinants of the  $T_s$ /VI relationship in addition to the vegetation fractional cover and scene component thermal properties, as the synoptic state of the atmosphere ( $T_{\text{air}}$  and vapour pressure deficit), the net radiation ( $R_n$ ), atmospheric forcing, soil surface moisture and the vegetation physiological activity. Lambin and Ehrlich (1996) commented specifically on the difficulty in determining the specific influence of any single parameter, since they believed this to be dependent on land-cover type, the climatic and surface moisture condition, and the other specific study area characteristics (eg, soil type, land-form, local climate, spatial heterogeneity in surface attributes, latitude).

Following this summary of the drivers of the  $T_s$ /VI feature space relationship, in

the following section a comprehensive and systematic review of the remote sensing methods employed in the retrieval of spatially explicit maps of land surface energy fluxes and surface soil moisture using this approach is made available.

### III Overview of remote sensing based $T_s$ /VI methods for the retrieval of land surface energy fluxes and surface soil moisture

A number of discrete methodologies have been developed to permit retrieval of land surface energy fluxes and surface soil moisture content from the information contained in a satellite-derived  $T_s$ /VI scatterplot. The remaining part of the present article deals exclusively with this topic, and provides an inclusive review of the key approaches employed. It is generally difficult to definitively classify these methods, since their complexity depends on the different types of assumptions and principles involved as well as the type of data required. For convenience and efficiency we review the different methods classed on the basis of the exact thermal and optical spectral range data used to form the two-dimensional scatterplot:

- (1) surface temperature ( $T_s$ ) and simple vegetation index (VI);
- (2) surface temperature ( $T_s$ ) and albedo;
- (3) surface-air temperature difference and vegetation index;
- (4) the day-night surface temperature difference and vegetation index;
- (5) coupling of the  $T_s$ /VI feature space data with a Soil Vegetation Atmosphere Transfer (SVAT) model.

A summary of the comparative performance metrics of these different methodologies is offered in Table 1.

*1 Methods based on the surface temperature ( $T_s$ ) and simple vegetation index (VI) scatterplot*  
Price (1990) appears to have been first to propose the idea of deriving spatially explicit

**Table 1** Summary of the major  $T_s/VI$  studies reviewed herein

| Study  | Accuracy reported   | Study location               | Sensor used                                  |
|--|---|------------------------------|--|
| <b>(1) Methods based on <math>T_s/VI</math> scatterplot</b>  |   |                              |  |
| Price (1990)   | No actual comparisons versus field data   | Southern Great Plains, USA   | AVHRR  |
| Jiang and Islam (1999)   | RMSD of $36.5 \text{ Wm}^{-2}$ in LE, bias of $\sim 12 \text{ Wm}^{-2}$ , R of 0.47   | Southern Great Plains, USA   | AVHRR  |
| Jiang and Islam (2001)   | For LE: RMSD of $85.3 \text{ Wm}^{-2}$ , bias of $9.0 \text{ Wm}^{-2}$ and R ranging between 0.16 and 0.67  | Southern Great Plains, USA   | AVHRR  |
| Sandholt <i>et al.</i> (2002)  | R <sup>2</sup> varied from 0.23 to 0.81 in comparisons done versus simulations  | West Africa                  | AVHRR  |
| Nishida <i>et al.</i> (2003a)  | In EF: RMSD of 0.17, bias of 0.01, R <sup>2</sup> of 0.71<br>In LE: RMSD of $45.06 \text{ Wm}^{-2}$ , bias of $5.59 \text{ Wm}^{-2}$ , R <sup>2</sup> of 0.86 | continental USA              | MODIS  |
| Wan <i>et al.</i> (2004)   | R <sup>2</sup> for VTCI varied from $-0.160$ to $0.626$ with a mean R <sup>2</sup> of 0.23  | Southern Great Plains, USA   | MODIS  |
| Parida (2006)  | R <sup>2</sup> for dry and wet edges reported to vary between 0.90 to 0.99  | India                        | MODIS  |
| <b>(2) Methods based on the <math>T_s/\text{albedo}</math> scatterplot</b>                         |   |                              |  |
| Roerink <i>et al.</i> (2000)   | Maximum relative difference of 8% in EF<br>Generally, method systematically overestimated both LE and H   | Italy                        | Landsat TM data                              |
| Gomez <i>et al.</i> (2005)   | RMSD of $90 \text{ Wm}^{-2}$ and $1 \text{ mm day}^{-1}$ in instantaneous and daily total LE, respectively  | Alpilles ReSeDA site, France | airborne PoLDER and TIR (20 m)               |
| Sobrino <i>et al.</i> (2005)   | RMSD of $1 \text{ mm day}^{-1}$ or better in daily LE   | Spain                        | DAIS airborne (2–30 m)                       |
| Sobrino <i>et al.</i> (2007)   | RMSD of $1.4 \text{ mm day}^{-1}$ in daily LE   | Spain                        | AVHRR  |
| <b>(3) Methods based on surface-air temperature difference versus vegetation index scatterplot</b> |   |                              |  |
| Moran <i>et al.</i> (1994; 1996)   | RMSD of $\sim 30 \text{ Wm}^{-2}$ in LE estimation  | Arizona, USA                 | Airborne MMR, Landsat TM, field spectrometer |
| Li and Lyons (1998)  | RMSD of the order of $40 \text{ Wm}^{-2}$ in LE estimation  | Southwestern Australia       | airborne data from BuFex experiment          |
| Jiang and Islam (2003)   | EF estimates: RMSD of 0.12, bias of $-0.081$ , R of 0.55<br>LE estimates: RMSD of $58.6 \text{ Wm}^{-2}$ , bias of $-42.4 \text{ Wm}^{-2}$ , R of 0.89        | Southern Great Plains, USA   | AVHRR  |
| Venturini <i>et al.</i> (2004)   | In EF comparisons: RMSD varied from 0.08 to 0.19 (mean value 0.13) and R <sup>2</sup> ranged from 0.4 to 0.7 (mean value 0.58)                                | South Florida, USA           | MODIS, AVHRR                                 |

|  |  |                            |   |
|--|--|----------------------------|---|
| Batra <i>et al.</i> (2006)   | For LE: RMSD ranged from 51 to 56 $Wm^{-2}$ , biases ranged from $-29$ to 12 $Wm^{-2}$ and $R^2$ ranged from 0.79 to 0.84  | Southern Great Plains, USA | MODIS, AVHRR  |
| Stisen <i>et al.</i> (2008)  | RMSD of 0.13 and $R^2$ of 0.63 for EF and RMSD of 41.45 $Wm^{-2}$ and $R^2$ of 0.66 for the LE   | South Senegal, Africa      | MSG SEVIRI  |
| <b>(4) Methods based on day-night temperature difference versus vegetation index scatterplot</b>       |  |                            |   |
| Tan (1998), Chen <i>et al.</i> (2002)  | % errors ranged from 2.8 to 23.9% in the estimation of daily LE fluxes RMSDs varying from 3.08 to 5.74 $mm\ day^{-1}$  | South Florida, USA         | AVHRR   |
| Wang <i>et al.</i> (2006)  | Mean relative accuracy of 17% in the estimation of EF with $R^2$ ranging from 0.34 to 0.61 and bias ranging from $-0.03$ to $-0.002$                                   | Southern Great Plains, USA | MODIS   |
| <b>(5) Methods based on the coupling between the <math>T_s</math>/VI scatterplot with a SVAT model</b> |  |                            |   |
| Carlson <i>et al.</i> (1990)   | No results were provided comparing fluxes/ $M_0$   | HAPEX experiment, France   | NS001 airborne simulator  |
| Gillies and Carlson (1995)   | Only visual/qualitative comparisons of derived $M_0$ were performed  | Newcastle Upon Tyne, UK    | AVHRR   |
| Carlson <i>et al.</i> (1995a)  | $M_0$ poorly correlated to both ground and microwave observations from PBMR sensor, $M_0$ -predicted reported consistently higher                                      | Pennsylvania, USA          | Airborne data from NS001 ( $\sim 30$ m)   |
| Gillies <i>et al.</i> (1997)   | Standard errors in LE and H between 25 and 55 $Wm^{-2}$ or about $\pm 10\%$ and $\pm 30\%$ , respectively, of the magnitude of the fluxes, and for $M_0$ about 16%     | Kansas and Arizona, USA    | High resolution airborne data from the NS001, (FIFE and MONSOON 90 field campaigns) |
| Capehart and Carlson (1997)  | Mean standard error and mean $R^2$ in LE estimation of 34.73 $Wm^{-2}$ and 0.94, respectively  | Mahantango, USA            | AVHRR   |
| Crombie <i>et al.</i> (1999)   | Mean standard error and mean $R^2$ in H estimation of 39.61 $Wm^{-2}$ and 0.83, respectively   | Nile delta, Egypt          | AVHRR   |
| Margulis <i>et al.</i> (2005)  | RMSD and $R^2$ in $M_0$ comparisons ranged between 0.15 and 0.19 and 0.27 and 0.44, respectively   | Kansas city, USA           | FIFE data (mainly <i>in situ</i> )  |
| Brunsell and Gillies (2003)  | $M_0$ study with fliarisis ( $R^2=0.37$ )  | Southern Great Plains, USA | TMS/TIMS airborne (12 m) and AVHRR (1 km)   |
| Chauhan <i>et al.</i> (2003)   | RMSD of 82 $Wm^{-2}$ and 68 $Wm^{-2}$ for LE and H, mean biases 56 and $-28\ Wm^{-2}$ , respectively   | Southern Great Plains, USA | (SSM/I) (25 km); AVHRR (1 km)   |
|  | Agreement within $\sim 15\%$ for both LE and H for the high-resolution data. Agreement in the satellite data was poor (50% difference for LE and 77% difference for H) |                            |   |
|  | RMSD $\sim 5\%$ in the estimation of $M_0$ .   |                            |   |



maps of LE fluxes via a mathematical description of how remotely sensed measurement points fell within the  $T_s$ /NDVI triangular space. His method required independent estimates of the LE fluxes for a site with full vegetation cover, and for dry and wet bare soil, corresponding to the extremities of the  $T_s$ /NDVI envelope. These values were then linked to a linear mixture modelling scheme to solve for LE fluxes in the interior of the  $T_s$ /NDVI pixel envelope. Using data from the AVHRR sensor, Price (1990) demonstrated for a site in Southern Great Plains (SGP), USA, that reasonable estimates of the instantaneous LE flux could be derived from the  $T_s$ /NDVI scatterplot using this approach, but no quantitative independent validation was available at that time. An important limitation of the method was the requirement for independent estimates of LE fluxes to be available for examples of fully vegetated and bare soil areas, although the areas used did not necessarily need to be identifiable in the satellite imagery.

Subsequent to the initial work of Price (1990) no significant progress in this type of approach was made for almost a decade. Jiang and Islam (1999; 2001) then suggested an alternative technique for the estimation of regional LE, based on the combination of the  $T_s$ /NDVI scatterplot and a simplified form of the Priestley-Taylor equation for LE fluxes, where some parameters of the latter were derived from the  $T_s$ /NDVI pixel envelope. A key assumption was that areas with extreme LE fluxes could be identified from the remotely sensed data as pixels with high surface soil moisture and consequently low surface albedo and relatively low  $T_s$ . Verification of the scheme to estimate instantaneous LE flux using AVHRR data for Southern Great Plains (SGP), USA, showed a RMSD of  $36.5 \text{ Wm}^{-2}$ , a bias of  $-12 \text{ Wm}^{-2}$  and a correlation coefficient of 0.47 when compared to direct field observations. Jiang and Islam (2001), using an increased AVHRR data set covering the same region (ie, the SGP), showed that the method provided estimates of the LE

fluxes with a high RMSD of  $85.3 \text{ Wm}^{-2}$ , a bias of  $9 \text{ Wm}^{-2}$  and a correlation coefficient between the days compared ranging from 0.16 to 0.67. The relative independence of their method from site-specific tuning of model parameters, offering the potential for perhaps operational use over large areas, was argued by the authors to be a key advantage. However, they accepted the criticism that the Priestley-Taylor type formulation does not explicitly account for the aerodynamic and physiological effects of the surface.

Sandholt *et al.* (2002) proposed a technique for estimating surface soil moisture content by linking the  $T_s$ /VI scatterplot with an index, which they termed the Temperature-Vegetation-Dryness-Index (TVDI). The principles of their model are depicted in Figure 2. Briefly, a linear empirical relationship between  $T_s$ , NDVI and the TVDI was proposed by the authors to be used to invert for surface soil moisture, with the assumption that soil moisture is the main source of variation for  $T_s$  and that TVDI is related to surface soil moisture due to changes in thermal inertia and evaporative control (ie, both evaporation and transpiration) on the available energy (ie,  $R_n - G$ ). Comparison of the surface soil moisture content output of the approach applied to AVHRR data to simulated soil moisture maps produced by the MIKE SHE distributed hydrological model (Abbott *et al.*, 1986) at a test site in West Africa indicated spatially similar soil moisture spatial patterns ( $R^2 = 0.70$ ). Intercomparisons, however, were performed between data that had been obtained at dissimilar spatial resolutions (MIKE SHE grid cell output at  $4 \times 4 \text{ km}$  and AVHRR at  $1 \times 1 \text{ km}$ ) and soil water depths. One of the most attractive elements of the method was, however, its independence from the types of ancillary data previously required when defining and interpreting the limits of the  $T_s$ /NDVI space. None-the-less, the requirement for the full range of variability in land surface conditions to be present within the scatterplot limited the methods applicability in more homogeneous regions.

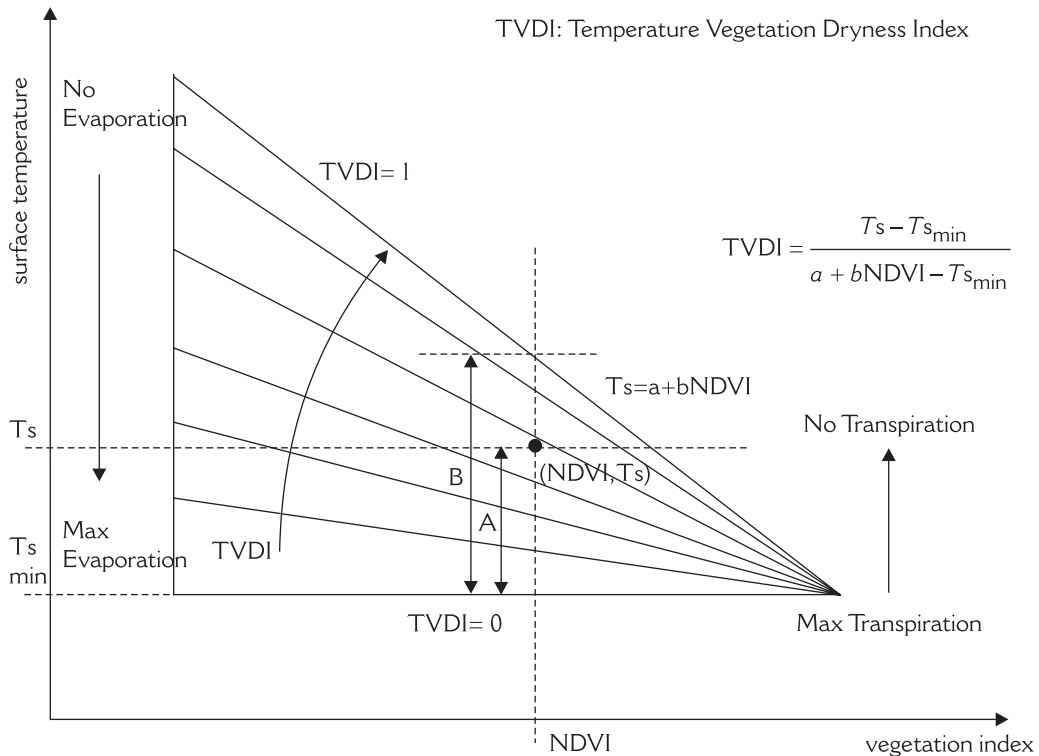


**Figure 2** Computation of the Temperature Vegetation Dryness Index (TVDI) for each pixel within the NDVI/ $T_s$  feature space domain proposed by Sandholt *et al.* (2002).  $T_s$  denotes the land surface temperature, while NDVI is the normalized difference vegetation index that has been shown to be related to green vegetation cover (Choudhury *et al.*, 1994). One example pixel characterized by particular  $T_s$  and NDVI measures is located at the intersection of the dashed lines. The  $a$  and  $b$  are the parameters defining the dry edge modelled as a linear fit to satellite data that is estimated from a region large enough to encompass a full variation in surface soil moisture conditions.  $A$  and  $B$  are the lines from which TVDI is estimated for a given pixel in the  $T_s/VI$  domain  
 Source: Adapted from Sandholt *et al.* (2002).

Nishida *et al.* (2003a; 2003b), again based on the  $T_s/VI$  scatterplot concept, proposed the operational retrieval of daily and eight-day composite Evaporative Fraction (EF) maps (EF defined as  $LE/(LE+H)$  or equally as the ratio of LE flux to the available energy – see Shuttleworth *et al.*, 1989) from Moderate Resolution Imaging Spectroradiometer (MODIS) data. The scheme proposed retrieval of LE flux based on separate estimates from the bare soil and vegetation components, and the  $T_s/VI$

scatterplot was used specifically to retrieve  $T_{air}$ , soil temperature and soil maximum temperature. The methodological details are described in Nishida *et al.* (2003b), while Nishida *et al.* (2003a) provide an evaluation of the algorithms performance at selected Ameriflux fluxtower sites using both NOAA AVHRR and Terra-MODIS satellite data, demonstrating satisfactory results in the comparisons of both EF (RMSD = 0.17, bias = 0.01,  $R^2 = 0.71$ ) and instantaneous LE fluxes (RMSD =  $45.06 \text{ Wm}^{-2}$ , bias =  $5.589 \text{ Wm}^{-2}$ ,

$R^2 = 0.86$ ). Nevertheless, it was noted that their proposed scheme was somewhat computationally expensive compared to other related methods. In addition, use of the eight-day composite EF product was the subject of some scepticism due to the potential impact of cloud cover and the influence of combining data from different overpasses to obtain the components of the  $T_s$ /VI pixel envelope (eg, Jiang *et al.*, 2004). These points may help explain why the Nishida *et al.* (2003a; 2003b) approach has not been applied operationally in the MODIS processing chain as yet.

From a different perspective, Wan *et al.* (2004) proposed a technique for retrieving information on the spatial variation in drought condition (a parameter highly correlated to the soil moisture content) via the  $T_s$ /NDVI scatterplot, terming this the Vegetation Temperature Condition Index (VTCI). Wan *et al.* (2004) suggested that VTCI isolines can be drawn in the NDVI versus  $T_s$  scatterplot, with the upper limit of the triangle representing the NDVI maximum and the lower limit representing  $T_s$  at maximum NDVI (Figure 3). According to the authors, the dry and wet edges could be estimated from the scatterplot using linear regression, and the derived equations could then be used for computing VTCI at each pixel, following the methodology detailed by Wan *et al.* (2004). Authors demonstrated the potential of their method for near-real time drought monitoring for a test site located in the USA using Terra-MODIS 16-day composite data ( $R^2$  for VTCI varied from  $-0.160$  to  $0.626$  with a mean  $R^2$  of  $0.23$ ). Following Wan *et al.* (2004), Parida (2006) used the eight-day composite Terra-MODIS NDVI and surface kinetic temperature products over a test region in India to show the existence of a distinct positive correlation between the Crop Moisture Index (CMI) and VTCI during the most prominent periods of drought ( $R^2$  for dry and wet edges reported to vary between  $0.90$  and  $0.99$ ). Parida (2006) in the same study also demonstrated the ability of VTCI to detect drought stress, by relating

the VTCI-based drought duration with crop yield information. Despite these encouraging results, their approach was dependent on a full, or at least very wide-ranged, variation in both NDVI and surface moisture condition within the study region, a requirement that generally cannot always be satisfied, particularly over more homogeneous areas.

## 2 Methods based on the surface temperature ( $T_s$ ) and albedo scatterplot

A number of studies have demonstrated a correlation between  $T_s$  and albedo for areas with spatially invariant atmospheric conditions, suggesting that the derived relationships can be applied to determine the effective land surface properties (Menenti *et al.*, 1989; Bastiaanssen, 1995). On this basis, Roerink *et al.* (2000) were the first to propose a scheme for deriving spatially explicit surface energy fluxes from remote sensing, based on the spatial variation of  $T_s$  and broadband albedo (rather than VI) and simple satellite-based estimates of  $R_n$  and  $G$  (Figure 4). In their method, which was termed the Simplified Surface Energy Balance Index (S-SEBI), for a given surface albedo, the variation of  $T_s$  between the wet and dry 'edges' was mainly related to variations in soil surface water availability. These data were then used to partition the available energy into  $H$  and  $LE$ , according to the actual temperature of the surface, assuming conditions of constant global radiation and  $T_{air}$ . Details of their proposed model can be found in Roerink *et al.* (2000). Verification of the method for one test region in Italy using field observations and Landsat TM data, showed a maximum relative difference of 8% in EF, but predicted instantaneous  $LE$  and  $H$  fluxes were reported to be systematically overestimated (Roerink *et al.*, 2000).

Gomez *et al.* (2005) recently extended the S-SEBI concept of Roerink *et al.* (2000) to retrieve daily total  $LE$  fluxes via an integration of the instantaneous  $LE$  fluxes over the whole day, and conversion into a daily value by accounting for the heat of vaporization.

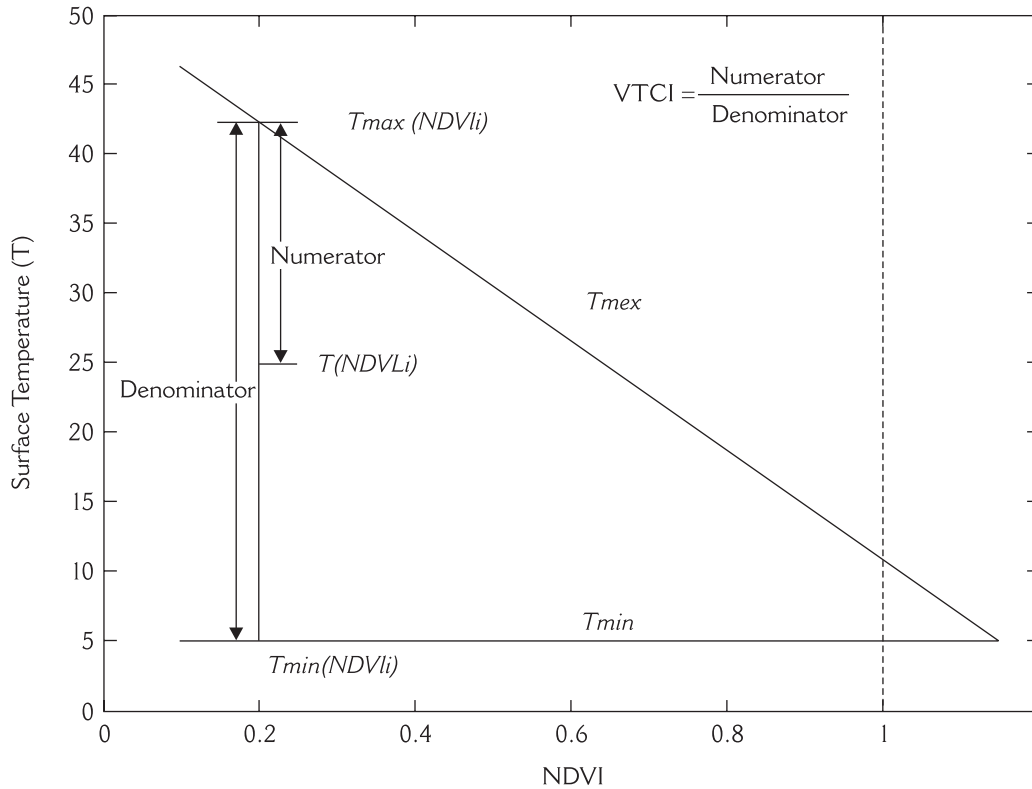


**Figure 3** Illustration of the physical principles of the Vegetation Temperature Condition Index (VTCI) method proposed by Wan *et al.* (2004). VTCI is defined as the ratio of  $T_s$  differences among pixels with a specific NDVI value over a sufficiently large study area. The vertical dashed line represents the theoretical maximum NDVI value ( $NDVI \sim 1.0$ ).  $T_{max}$  and  $T_{min}$  represent the maximum and minimum surface temperatures, respectively, viewed by Wan *et al.* (2004) as the warm and cold edges, respectively. The equations for the warm and cold edges estimated from the scatterplot using linear regression are used subsequently for the computation of VTCI for each pixel following the equations detailed in Wan *et al.* (2004)

Source: Adapted from Wan *et al.* (2004).

Gomez *et al.* (2005) based their approach on the assumption that the EF operating at the scale of one day is similar to the instantaneously derived value retrieved at the time of the remote sensing data acquisition. The authors performed a verification of their method at a test site in the Alpillés ReSeDA experimental area using data collected from the airborne PoLDER (Polarization and Directionality of Earth Reflectance) instrument and a thermal infrared camera at 20 m

spatial resolution. Results indicated a RSMD of  $90 \text{ Wm}^{-2}$  and  $1 \text{ mm day}^{-1}$  in the estimates instantaneous and daily total LE fluxes, respectively. Sobrino *et al.* (2005) provided a further evaluation of the Gomez *et al.* (2005) methodology over a mainly agricultural site in Spain, using high spatial resolution ( $\sim 2\text{--}30 \text{ m}$ ) Digital Airborne Imaging Spectrometer (DAIS) imagery. Results suggested that the methodology was able to provide estimates of regional daily total LE flux to an accuracy

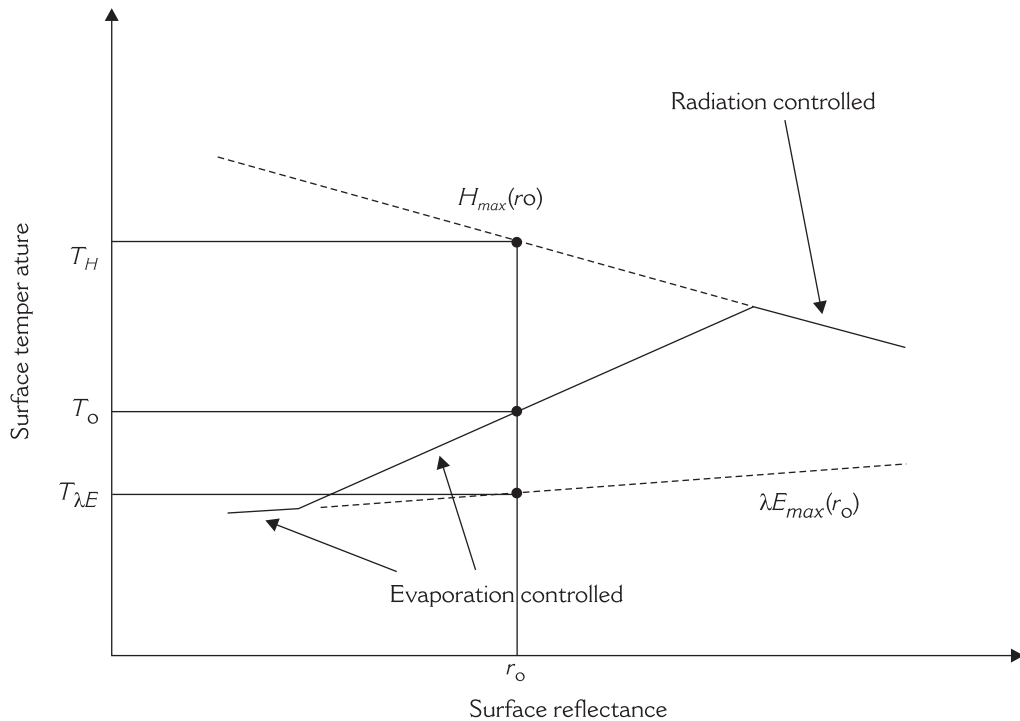


**Figure 4** The concept of  $T_s$ /albedo scatterplot method for the retrieval of instantaneous and daily LE fluxes, proposed, for example, by Roerink *et al.* (2000).  $\lambda E_{\max}(r_o)$  represents the line of pixels showing the maximum LE flux (ie, pixels from the wetter parts of the image) whereas  $H_{\max}(r_o)$  represents the line of pixels exhibiting the driest surfaces)

Source: Adapted from Roerink *et al.* (2000).

of better than  $1 \text{ mm day}^{-1}$ . Sobrino *et al.* (2007) investigated the use of the Gomez *et al.* (2005) method with coarse spatial resolution AVHRR data using the same agricultural site as the Sobrino *et al.* (2005) study. A RMSD of  $1.4 \text{ mm day}^{-1}$  in the estimation of daily LE flux was reported in their study. Given the high temporal resolution of the AVHRR sensor, Sobrino *et al.* (2007) were also able to demonstrate an ability to provide regular monitoring of the daily total LE fluxes. A major advantage of the Roerink *et al.* (2000) and Gomez *et al.* (2005) method includes their being independent of additional meteorological data, provided that surface hydrological extremes are present within

the image under study. Also, an important point to note is that the method assumes that the extreme temperatures for the wet and dry conditions vary with changing surface reflectance. This contrasts with the other  $T_s$ /VI methods reviewed thus far which attempt to determine a fixed temperature for the extreme wet and dry conditions, representative of the entire area of interest and/or for each land-use/cover class. Yet the Gomez *et al.* (2005) approach is characterized by two main disadvantages that may restrict its use in more operational applications. These are the requirement to have  $T_s$  measurements for both bare soil and full vegetation cover, and the assumption

of homogeneous atmospheric conditions (mainly global radiation, wind speed and  $T_{\text{air}}$ ) over the entire studied area.

**3 Methods based on surface-air temperature difference and vegetation index scatterplot**  
Moran *et al.* (1994) introduced a concept termed the ‘vegetation index–temperature (VIT) trapezoid’ for the estimation of LE fluxes using the  $T_s/VI$  domain in areas of partial vegetation cover. Briefly, the Moran *et al.* (1994) methodology was based on the use of the Crop Water Stress Index (CWSI) of Jackson *et al.* (1981) and a new index defined as the Water Deficit Index (WDI). These indices were linked to computed

values of the four vertices of the  $T_s/VI$  trapezoid and subsequently related to the retrieval of LE for any point within the trapezoid (Figure 5). The authors demonstrated the method for an agricultural site in Arizona, USA, using both model simulations and Modular Multispectral Radiometer (MMR) airborne data. However, no quantitative intercomparisons were made to independent measurements. Later, Moran *et al.* (1996) verified the approach over a semi-arid grassland site in Arizona, USA, using ground-based measurements of surface reflectance and temperature obtained during the Walnut Gulch (WG) field campaign (Kustas *et al.*, 1991). Results from the point

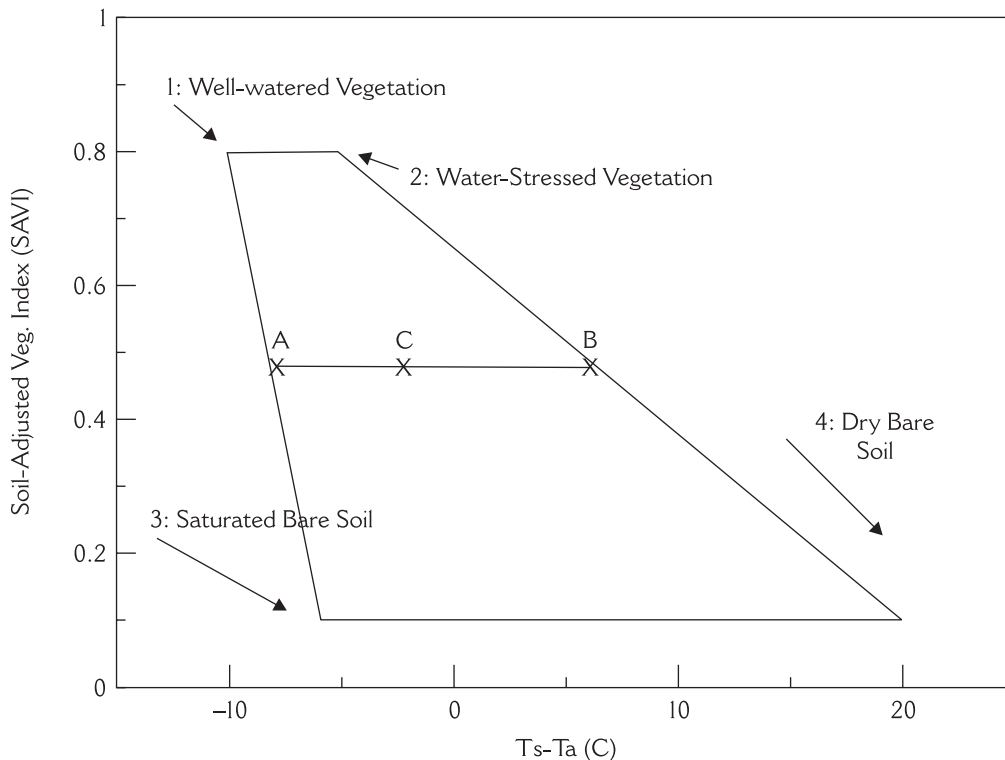


**Figure 5** Illustration of the principles of the trapezoidal method of Moran *et al.* (1994) for the estimation of the instantaneous LE fluxes from the  $(T_s - T_{\text{air}})/VI$  domain.  $T_s$  is the land surface temperature and  $T_a$  is here the surface air temperature. According to the authors, having a measurement of  $(T_s - T_a)$  at any point C inside the trapezoid allows one to equate the ratio of actual to potential LE with the ratio of the distances CB and AB

Source: Adapted from Moran *et al.* (1994).

comparisons showed a satisfactory RMSD of  $29 \text{ Wm}^{-2}$  from all days compared in the estimation of instantaneous LE fluxes, though, with a consistent overestimation at most sites. Subsequently, Moran *et al.* (1996) then demonstrated use of the technique with Landsat TM data for a series of grassland sites within their study region, but analysis was mainly based on image histograms and visual comparisons of the satellite-derived fluxes and those of topography and SAVI, rather than quantitative measures.

Li and Lyons (1998) performed an inter-comparison of three remote sensing-based LE methods, including that of Moran *et al.* (1994; 1996). Their study was carried out using airborne data from the Bunny Fence Experiment (BuFex) conducted in Western Australia (Lyons *et al.*, 1993). Specifically with regards to the performance of the Moran *et al.* (1994; 1996) method, their analysis reported an average Root Mean Squared Difference (RMSD) over native vegetation of the order of  $40 \text{ Wm}^{-2}$  in instantaneous LE flux estimation versus ground observations. The authors concluded that the Moran *et al.* (1994) method is suitable for regional-scale applications, but also underlined that application of the method is restricted at locations without  $T_{\text{air}}$  measurements or where it exhibits large spatial variations. The most significant advantage of the Moran *et al.* (1996) 'trapezoid' approach appears to be related to the use of the WDI index, which allowed relatively easy calculation of instantaneous LE fluxes within the trapezoidal domain for both heterogeneous and homogeneous surfaces, in contrast with the CWSI that was applicable only to more homogeneous areas. Another advantage was the relatively limited dependence on *in situ* observations, namely  $R_n$ , vapour pressure deficit, wind speed and  $T_{\text{air}}$ . Nevertheless, the accuracy of the approach was strongly influenced by the quality of these input parameters.

Jiang and Islam (2003) proposed a different scheme for the retrieval of the LE

fluxes, based on a modification of the method originally proposed by Jiang and Islam (1999), with the main difference being the use of the  $T_s - T_{\text{air}}$  measure (also known as DT) – in place of  $T_s$ . The authors argued that locations where  $DT = 0$  always represent the true cold edge of the triangular space, where H flux is negligible (near zero) and LE flux is equal to the available energy ( $R_n - G$ ), ie, where the  $EF = 1.0$ . Another difference with regard to the Jiang and Islam (1999) method was related to the use of the  $F_r$  parameter introduced by Choudhury *et al.* (1994) as a proxy for vegetation cover, instead of the basic NDVI. Jiang and Islam (2003) compared the output from their method to that from the commonly used aerodynamic resistance energy balance approach, using AVHRR data and ground observations collected from the SGP region (USA). In terms of the EF estimates, RMSD and bias were 0.12 and  $-0.081$ , respectively, and a correlation coefficient of 0.55 was reported. Analogous comparisons of the LE flux estimates showed an RMSD and bias of 58.6 and  $-42.4 \text{ Wm}^{-2}$ , respectively, and a correlation coefficient of 0.89. Jiang and Islam (2003) regarded an important advantage of their method as the fact that it was not too dependent on the absolute accuracy of the  $T_s$  measures, because  $DT$  equal to zero in their proposed scheme always represented the true cold edge of the triangular space where  $EF$  equals zero. The approach also appeared less complex to implement than that of Moran *et al.* (1994; 1996). Nonetheless, as with the methods described previously, the Jiang and Islam (2003) method also assumes a linear variation in  $EF$  across the triangular/trapezoid domain of ( $F_r$ ,  $DT$ ) feature space for each vegetation fraction ( $F_r$ ) class.

Venturini *et al.* (2004) for a test region over South Florida demonstrated the use of the Jiang and Islam (2003) method for the estimation of regional scale maps of  $EF$  using MODIS and AVHRR. In the same study, the authors also demonstrated that the two sensors produced comparable estimates of

EF, despite variations in their respective NDVI and  $T_s$  measures resulting from differences in the sensor spectral response functions. Over different days the RMSD in EF varied from 0.08 to 0.19 (mean value 0.13) and  $R^2$  ranged from 0.4 to 0.7 (mean value 0.58). Findings from their study added to the suggestion of Jiang and Islam (2003) that the method was relatively insensitive to sensor-specific changes in  $T_s$  induced by the used of different imaging sensors. Batra *et al.* (2006) used MODIS and AVHRR data to demonstrate the utility of the Jiang and Islam (1999; 2003) method for the production of spatial maps of EF over large heterogeneous areas for selected days in the SGP region (USA). Their analysis showed approximate RMSD values for the inverted LE fluxes of 53, 51 and 56  $Wm^{-2}$  and a correlation coefficient of 0.84, 0.79 and 0.77 from the MODIS, NOAA-16 and NOAA-14 sensors, respectively.

Recently, Stisen *et al.* (2008), using data from METEOSAT SEVIRI and ground observations from a test site in South Senegal, West Africa, proposed that the use of the  $(T_s - T_{air})$  measure in the Jiang and Islam (2003) approach be substituted by either  $T_s$  recorded at 12:00 local time or by the surface temperature difference ( $dT_s$ ) calculated between 12:00 and 8:00 local time. A further difference, compared to the original Jiang and Islam (2003) approach, included a non-linear interpretation of the  $T_s$ /VI domain, essentially based on a non-linear interpolation of ' $\phi$ ' parameter with respect to NDVI (' $\phi$ ' representing the complex effects of the 'A' and 'B' parameters of the Priestley-Taylor equation). Stisen *et al.* (2008) results indicated a very good agreement with ground measurements of EF (RMSD of 0.13 and  $R^2$  of 0.63) and instantaneous LE fluxes (RMSD of 41.45  $Wm^{-2}$  and  $R^2$  of 0.66). However, a weakness of their proposed scheme, recognized by the authors, was the fact that the method did not allow for the presence of water stress over full vegetation cover where EF is zero along the observed dry edge.

However, a major advantage of the Stisen *et al.* (2008) approach included the fact that it was rather independent of ancillary data and was demonstrably usable with high temporal resolution geostationary data, which allowed for the monitoring of the diurnal temperature variation. Also, compared to all studies reviewed so far, it should be noted that the Stisen *et al.* (2008) approach was the first to suggest a non-linear interpretation of the  $T_s$ /VI domain, which is probably a more realistic representation of the relationships between the biophysical properties encapsulated in the  $T_s$ /VI scatterplot compared to a basic linear interpretation.

#### 4 Methods based on day-night temperature difference and vegetation index scatterplot

Tan (1998) and Chen *et al.* (2002) were the first to propose that actual LE flux estimates can be retrieved from the scatterplot defined by the day-night  $T_s$  difference and the radiometric VI (Figure 6). The so-called Diurnal Surface Temperature Variation (DSTV) approach was based on findings from other studies that had demonstrated the existence of a strong relationship between the day and night-time  $T_s$  and the soil moisture/thermal inertia (van de Griend *et al.*, 1985; Jordan and Shih, 2000). The proposed technique was based on first implementing a simple linear mixture model on the DSTV/VI domain to determine the fractional contributions of the values for each pixel from vegetation, dry and wet soil surfaces. Subsequently, a new index, the vegetation and moisture coefficient (VMC), was expressed at each pixel as the sum of the weighted components of VMC from vegetation cover, dry soil and wet soil. The latter was used to determine the actual LE flux with the help of a Geographical Information System employed for the purpose of managing the data and computing the VMC parameter. The full workings are detailed in Chen *et al.* (2002) and validation of the approach over different land-use types for a test site in South Florida using AVHRR data



showed percentage errors in the estimation of LE fluxes of between 2.8 and 23.9%, with RMSDs varying from 3.08 to 5.74 mm day<sup>-1</sup>. An important advantage of the method was undoubtedly its requirement for only a small number of additional external parameters. Yet limitations included the constraint of assuming only three land-cover types in the mixture modelling scheme and the need for two satellite-derived  $T_s$  values (one daytime and one night-time). The further requirement that three distinct and homogeneous

land-use/cover types be identifiable at a sufficiently large spatial extent for VMC to be estimated potentially provided some restriction to the method's operational application.

Recently, Wang *et al.* (2006) proposed a different scheme to that of Chen *et al.* (2002) for the retrieval of EF. In their method, which was based on a modification of the Jiang and Islam (2003) approach, the authors suggested use of the day-night  $T_s$  difference and NDVI ( $\Delta T_s$ -NDVI), in place of the daytime

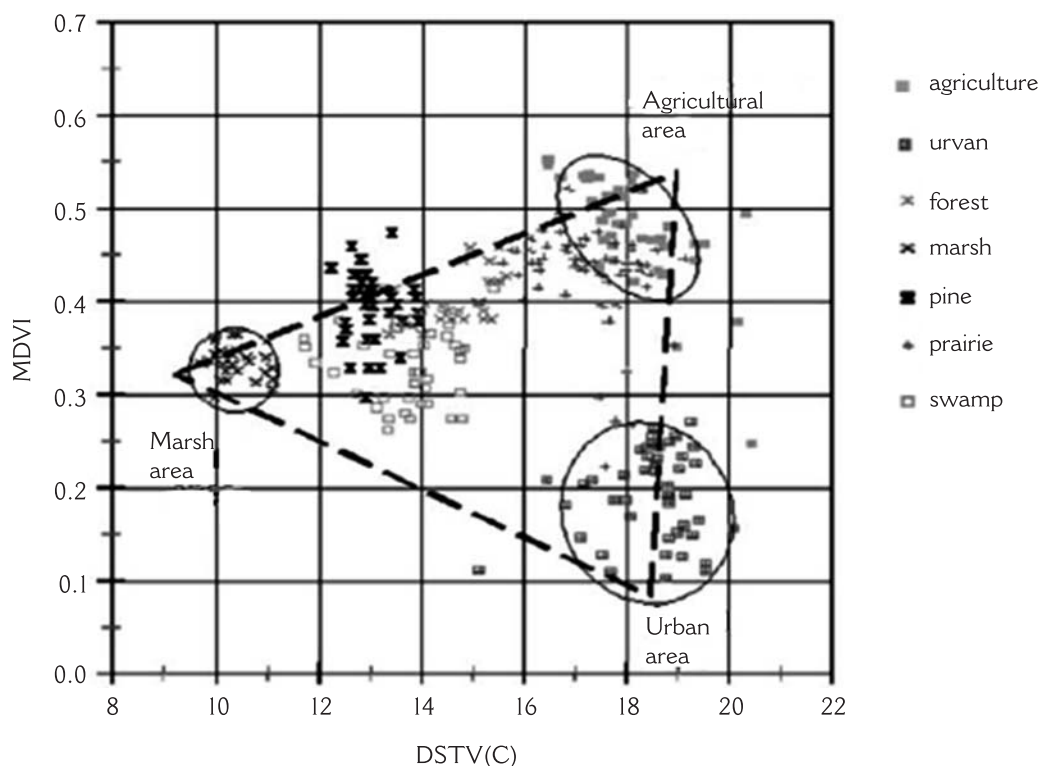


**Figure 6** Estimation of LE fluxes from the Diurnal Surface Temperature Variation (DSTV) approach of Chen *et al.* (2002), shown here for one of their example days. In this figure, pixels from seven land-use/cover types are mapped within the NDVI-DSTV feature space domain. Different areas (here marsh, agricultural and urban) were used to collect end-member spectra with which from a linear mixture modelling approach were determined the fractional contributions of the values for each pixel from vegetation, dry and wet soil surfaces that were then linked to the vegetation and moisture coefficient (VMC) index from which the actual LE fluxes were determined  
Source: Adapted from Chen *et al.* (2002).

$T_s$ . Full details of the scheme are provided in Wang *et al.* (2006) and validation at the SGP site (USA) using MODIS data showed a mean RMSD of 0.106, a bias of  $-0.002$  and an  $R^2$  of 0.61 in the estimation of EF as compared to ground measurements. These results were deemed satisfactory by the authors, taking into account the relative simplicity of the approach and the requirement for only a small number of ground measurements for its implementation. Nevertheless, a possible constraint – as in Chen *et al.* (2002) – is the requirement for spatial maps of surface temperatures under both consecutive daytime and night-time conditions, a requisite that obviously cannot be met by all sensors currently in orbit that are otherwise capable of being parameterized using the Wang *et al.* (2006) method.

#### 5 Methods based on the coupling of the $T_s$ /VI scatterplot with a SVAT model

An alternative approach to the estimation of surface energy fluxes and surface soil moisture content from  $T_s$ /VI feature space measures is focused on the coupling of these types of data with a Soil Vegetation Atmosphere Transfer (SVAT) model. A recent overview of the workings of this approach, often termed the ‘triangle’ method, which also included a reference to the method’s limitations, has been provided by Carlson (2007).

Based on previous research of Carlson *et al.* (1990), Gillies and Carlson (1995) introduced a new method for the retrieval of spatially distributed maps of soil surface moisture availability ( $M_o$ ) and land-atmosphere energy fluxes, which they termed the ‘triangle’ method. In this approach, the outputs from a SVAT model are coupled with the  $T_s$  and VI (here VI being replaced by  $F_r$ , as the latter is a physical quantity related directly to those used by the SVAT model) remotely sensed data via empirically derived correlations developed between the relevant input (eg,  $F_r$ ,  $M_o$ ) and output (eg, LE,  $T_s$ ) parameters of the physically derived model, parameterized

for the time of the satellite overpass. These correlations were in turn used with the remotely sensed values of, for example,  $F_r$  and  $T_s$ , to retrieve  $M_o$  and surface fluxes ( $R_n$ , LE and H) at each image pixel. In addition, Gillies and Carlson (1995) proposed a temperature normalization scheme, which offered the advantage of being able to better compare composite images from different days, since it minimized effects induced by differences in solar elevation angle, ambient temperature, surface roughness, radiometer drift and vegetation type. Gillies and Carlson (1995) demonstrated the technique using AVHRR images for the city of Newcastle Upon Tyne, UK (Figure 7). However, their analysis was based only on interpretations of the spatial patterns of the output  $M_o$ , which were reported to reflect those generally expected across the study area. Carlson *et al.* (1995a) provided a quantitative validation of the Gillies *et al.* (1995) method at a test site in Pennsylvania, USA, comparing the inverted maps of  $M_o$  and energy fluxes produced from the NS001 instrument to point observations and spatial maps of soil water content obtained from the Push Broom Microwave Radiometer (PBMR) obtained at  $\sim 450$  m spatial resolution. The authors generally reported low correlations between  $M_o$  derived from the PBMR and those estimated using the ‘triangle’ method, which they attributed to the rapid and irregular drying of the surface soil.

Gillies *et al.* (1997) proposed two major modifications in the implementation of the original ‘triangle’ method of Gillies *et al.* (1995). These included the use of an alternative algorithm for the calculation of  $F_r$  from NDVI (Choudhury *et al.*, 1994; Carlson and Ripley, 1997) and the use of a ‘stretching algorithm’ which aimed to shift the ‘triangle’ produced by the SVAT model to match that derived from the remote sensing data. Validation of the ‘triangle’ method performed by Gillies *et al.* (1997) again using airborne NS001 data showed standard errors in the order of  $\pm 10\%$  and  $\pm 30\%$  for the LE and H

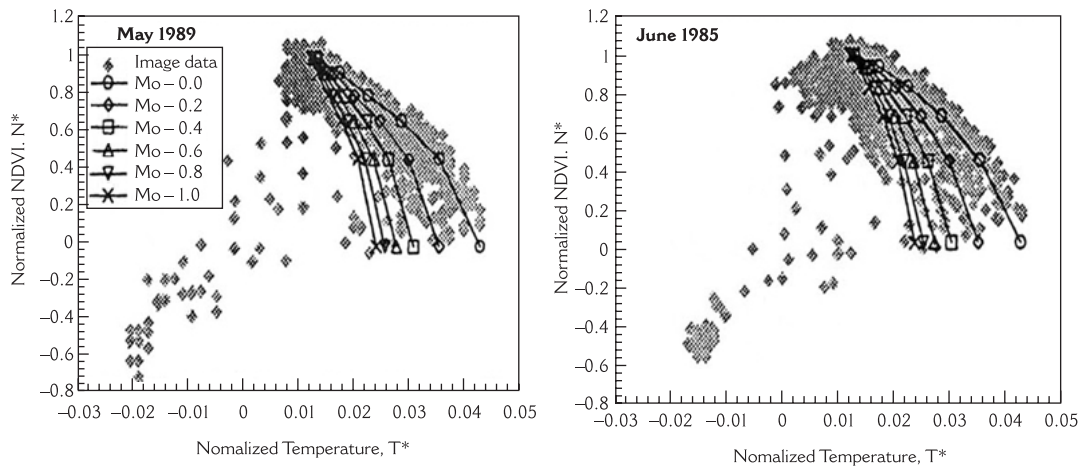


**Figure 7** Scatterplots of scaled NDVI (produced from a simple normalization of NDVI) versus normalized surface radiant temperature ( $T_s$ ) derived in the study of Gillies and Carlson (1995) for all the test days on which the method was implemented using NOAA AVHRR imagery. Isopleths of constant  $M_0$  derived from a series of SVAT model runs are superimposed on the pixel-derived data

Source: Adapted from Gillies and Carlson (1995).

fluxes and for  $M_0$  about 16% compared to observations collected from the FIFE (Sellers *et al.*, 1992) and MONSOON 90 (Kustas *et al.*, 1991) field campaigns. Their results, however, failed to prove the added value of the proposed stretching algorithm. Authors in the same study also proposed that, in addition to the instantaneous LE and H fluxes, the ratios of LE or H to  $R_n$  (LE/ $R_n$  or  $H_0/R_n$ ) can also be mapped inside the triangle domain. Use of these evaporative or sensible heat 'fractions', as they called these ratios, was argued to be close to a daytime average value of the LE and H fluxes, as these ratios are less dependent on the time of day and are also more intrinsically related to the surface soil moisture and vegetation cover. However, Gillies *et al.* (1997) failed to really provide any validation with regard to the ability of the 'triangle' method to resolve the daytime average land-atmosphere energy fluxes using these proposed ratios.

Capehart and Carlson (1997) evaluated the performance of the 'triangle' method for the Mahantango region in the USA,

using AVHRR data, compared to profiles of soil water content derived from the soil hydrology model of Capehart and Carlson (1994).  $M_0$  was reported to be consistently underestimated using the satellite-based approach, and agreement for different soil types was relatively low on a pixel-by-pixel basis, with  $R^2$  ranging from 0.27 to 0.44 and RMSD ranging from 0.15 to 0.19 vol vol<sup>-1</sup>. This low agreement was potentially attributed by the authors to the different soil layer depths that most influenced the 'triangle'-derived and model predicted results.

For the next eight years, a number of studies focused on demonstrating the use of the 'triangle' method in other applications, mainly the monitoring of urbanization (eg, Carlson and Sanchez-Azofeifa, 1999; Carlson and Arthur, 2000). Some researchers (eg, Owen *et al.*, 1998) also attempted to relate the temporal movement of particular image pixels within the  $T_s/F_r$  triangular envelope to changes in urbanization, expressed as increases in  $T_s$  as a result of the decline in both  $F_r$  and  $M_0$ . Certain studies also extended this

concept by relating the area of impervious surfaces and surface runoff (Carlson and Arthur, 2000) or the stormwater runoff (Arthur *et al.*, 2003) to the triangle domain. From a very different perspective, others (eg, Crombie *et al.*, 1999) attempted to relate the spatially explicit maps of  $M_o$  derived from the 'triangle' method to the prevalence of malaria and filariasis, since the mosquitoes that carry the related parasite require standing water to breed. However, the results unfortunately failed to show a very convincing correlation between filariasis infection rate and the retrieved  $M_o$  ( $R^2 = 0.37$ ).

Subsequent validation of the 'triangle' method was carried out more recently by Brunzell and Gillies (2003), who demonstrated the importance of scale in the study of processes concerning land-atmosphere interactions. The authors implemented the 'triangle' method using observations from the TMS/TIMS airborne imager (12 m spatial resolution) and the AVHRR (1 km spatial resolution), comparing their results to *in situ* observations from the SGP test site (USA). A particularly interesting characteristic of their study included demonstration of a procedure for using the SVAT model to interpolate the satellite-derived temperatures obtained from the two sensors at different overpass times, which allowed for improved comparison between the different data sets. Their analysis indicated a satisfactory agreement between the *in situ* measurements and results derived from the airborne data (within ~15% for both LE and H fluxes) but those from the satellite data were poor (50% difference for LE fluxes and 77% difference for H fluxes compared to both the observations and the airborne-derived measures).

Recently, Margulis *et al.* (2005) compared estimates of the instantaneous land-atmosphere energy fluxes output from the 'triangle' method to those produced by the variational data assimilation scheme of Caparrini *et al.* (2003). The two methods were also compared to observations from the First International Satellite Land Surface

Climatology Project (ISLSCP) Field Experiment (FIFE) for a grassland site in Kansas city, USA. Implementation of the 'triangle' method was conducted using the 'FR' model of Noilhan and Planton (1989) in place of the SVAT model of Gillies and Carlson (1995). Use of the 'FR' model was justified by the fact that it was able to be parameterized with exactly the same input parameters as required by the variational approach. Comparisons to the ground measurements showed a low agreement with those derived using the 'triangle' method (LE and H fluxes showing an average RMSD of 82  $Wm^{-2}$  and 68  $Wm^{-2}$ , respectively, in the hourly comparisons), whereas the variational method showed somehow better results (corresponding RMSD values 73 and 57  $Wm^{-2}$ ). Interpretations of the low level of agreement in the 'triangle' method results should take into account that the latter method was implemented in this study at a point scale using *in situ* and/or spatially averaged estimates of  $T_s$  taken during the FIFE experiment and a constant value for  $F_r$ , instead of actual satellite data to derive  $T_s$  and  $F_r$  and the triangle domain (personal communication, 2008).

Finally, Chauhan *et al.* (2003) proposed a variation of the 'triangle' method of Carlson *et al.* (1995a) and Gillies *et al.* (1995; 1997) for the operational retrieval of high-resolution (1 km) maps of surface soil moisture from the National Polar-orbiting Operational Environmental Satellite System (NPOESS). Their scheme was based on synergy between soil moisture estimates derived from the Conical Scanning Microwave Imager/ Sounder (CMIS) and the output of the 'triangle' method parameterized using data from the optical/infrared instrument Visible/Infrared Imager Radiometer Sensor Suite (VIIRS). Full details are provided in Chauhan *et al.* (2003) and an initial test of the technique for a grassland site in SGP (USA) using data from the Special Sensor Microwave Imager (SSM/I) (~25 km spatial resolution) and the AVHRR (1 km spatial resolution) showed

good performance. Soil moisture estimated from the 'triangle' approach by the AVHRR data was reported to agree reasonably well with the SSM/I low-resolution microwave-derived results in both magnitude and spatio-temporal pattern, with an RMSD of the order of 5%. However, it should be noted that Chauhan *et al.* (2003) discarded all highly vegetated pixels ( $NDVI > 0.4$ ), which are essentially those in which the uncertainty in the estimated  $M_o$  would be expected to be greater due to the perturbing influence of vegetation on the microwave signal. In June 2006 a decision was for the CMIS instrument on the planned NPOESS to be replaced by a less complex microwave instrument, the Microwave Imager Sounder (MIS), and the VIIRS and MIS instruments are now planned to be launched on the same NPOESS platform starting from 2016, followed by two further platform launches until approximately 2026.

#### IV Summary and outlook

This article has provided a systematic and relatively comprehensive review of the various methods employed for the estimation of fluxes of sensible (H) and latent (LE) heat, and surface soil moisture content, using various interpretations of the  $T_s/VI$  feature space scatterplots derived from remote sensing. General overviews of the use of other remote sensing based approaches for the estimation of LE and H fluxes and soil moisture are provided by others (see Moran *et al.*, 2004; Courault *et al.*, 2005; Carlson, 2007; Verstraeten *et al.*, 2008), and we have here only provided cursory reference to this group without an attempt to systematically organize and review them. We have, however, offered an overview of the main biophysical properties encapsulated the  $T_s/VI$  feature space in relation to the estimation of LE, H fluxes and  $M_o$ . Understanding of these is fundamental to the subsequent methods reviewed here.

The triangular space that emerges from such a scatterplot embodies a series of interesting

physical relationships which have been well documented by a range of studies over many years. The ability to relate the patterns encapsulated by the  $T_s/VI$  pixel envelope to key biophysical properties explains the large number of studies concerned with retrieving spatially explicit maps of H, LE fluxes and surface soil moisture content using information contained within the  $T_s/VI$  domain. As was clearly evidenced from the review of the  $T_s/VI$  methods undertaken here, the methods that exploit these relationships differ in their complexity and assumptions, as well as in their ancillary data requirements compared to other methods used in deriving these parameters from spaceborne data (eg, Norman *et al.*, 1995; Bastiaanssen *et al.*, 1998; Su, 2002; Mu *et al.*, 2007; Sanchez *et al.*, 2008; Anderson *et al.*, 2008). Some of the key advantages include their ability to be largely independent of ancillary surface and atmospheric information, to offer a relatively straightforward transformation between instantaneous flux estimates and daytime averages or totals, and to better deal with land surface heterogeneity. In our view, these are some of the main reasons justifying the continuing interest in these methods to date. Yet, as is evidenced by the performance summary included in Table 1, further steps appear necessary for the approaches to reach an absolute accuracy of  $50 \text{ Wm}^{-2}$  in terms of the H and LE fluxes, and 4% volume by volume for surface soil moisture content that has been reported as being required for operational applications by Seguin *et al.* (1999) and Calvet and Noilhan (2000).

A more detailed evaluation of the accuracy of the various  $T_s/VI$  approaches across a wide range of environmental, ecological and geographical locations, and with data taken at dissimilar spatial resolutions, is one of the major steps that is now required. Furthermore, the degree of empiricism/user subjectivity that is introduced by some of the methods reviewed here must be drastically reduced if they are to be very frequently applied or even considered for operational use. It also appears that to

best promote the use of  $T_s$ /VI approaches a number of technological/theoretical/practical hurdles must be overcome. Most specifically, an improvement in the general spatial and temporal resolution of the satellite instruments having specifications appropriate for use in the  $T_s$ /VI methods may be necessary in order to allow for more detailed study of the land-atmosphere energy fluxes and soil surface moisture. Indeed, some of the studies discussed here seem to have found good performance when using high spatial resolution airborne data but not coarse resolution (satellite) data (eg, Brunzell and Gillies, 2003; Gomez *et al.*, 2005). The development of techniques for improved implementation of these methods in areas subject to partially cloudy conditions and in areas not subject to the full range of surface variations would appear to be important, and (multispectral) methods that can be deployed to better estimate the parameters forming the scatterplot domain – particularly  $T_s$  – should probably be exploited. We have also seen that the linearity assumption with regard to the biophysical properties embedded in the  $T_s$ /VI scatterplot domain, adopted by most of the reviewed methods, is perhaps too much of an oversimplification. Studies such as Moran *et al.* (1994) and Sandholt *et al.* (2002) suggest that this may be a poor representation of the true physical processes relating the surface fluxes and soil moisture to locational changes in the ( $T_s$ /NDVI) feature space domain, and may especially be so for sparsely vegetated ecosystems. Mallick *et al.* (2009) summarize as the most important sources of uncertainty in the estimation particularly of soil moisture – that to some degree also apply to the surface energy fluxes estimation – from the  $T_s$ /VI domain the effects of viewing angle correction on  $T_s$  and VI, the account of overpassing cloud shadows, the potential errors in  $T_s$  and VI retrieval due to atmospheric and emissivity effects, the influence of soil water content in deeper layers, and the dependence of  $T_s$  and

VI on surface types since the latter is related to aerodynamic resistance.

Arguments for further work towards the development of methods for the operational retrieval of surface fluxes and soil moisture that take into consideration the parameters discussed here are potentially strengthened by launches of new satellite-based instruments having the potential to provide operational retrievals of these parameters. Key spaceborne instruments aiming to provide global data relevant to the estimation of the land-atmosphere energy fluxes and surface soil moisture content include the Microwave Imaging Radiometer using Aperture Synthesis (MIRAS) L-band microwave radiometer on board the European Space Agency (ESA) Soil Moisture and Ocean Salinity (SMOS) mission, as well as the Visible/Infrared Imager/Radiometer Suite (VIIRS) prepared by the NPOESS/NASA Preparatory Project (NPP) near polar orbiting satellites to be launched in 2010 and 2013, respectively. SMOS will provide observations relating directly to the surface soil moisture content, while VIIRS will be equipped with channels covering a wide range of spectral bands from the visible to the thermal IR (0.3–14 microns) at a spatial resolution of 400 m. VIIRS is of utmost interest in relation to the methods reviewed here and is planned to offer replacements for the observations currently taken by AVHRR and MODIS. However, it is worthwhile at this point to underline that no mission plan has been yet formalized regarding particularly the continuation of spaceborne thermal infrared data acquisitions at higher spatial resolutions at a global scale, as a succession of the LANDSAT and ASTER missions. As has already been pointed out by many (Li *et al.*, 2008; Anderson and Kustas, 2008), lack of availability of such data would result in a dramatic decrease in our ability to map the land surface processes occurring predominantly over highly fragmented regions, due to the incompatibility between spatial resolution and spatial heterogeneity. Yet we

await the implementations of the Chauhan *et al.* (2003) methodology for the operational retrieval of surface soil moisture using the synergy between VIIRS and the MIR instruments carried on the same NPOESS platform with interest.

#### *Acknowledgements*

This research was supported by funds obtained from the Greek Scholarships Foundation (IKY). This work was also supported, in part, by a grant from the US National Research Institute Competitive Grants Program (MASR-2004-00888).

#### **References**

- Abbott, M., Bathurst, J., Cunge, J. and O'Connell, P.E. Jr** 1986: An introduction to the European hydrological system – Systeme Hydrologique Europeen SHE 2: structure of a physically based distributed modelling system. *Journal of Hydrology* 87, 61–77.
- Anderson, M.C. and Kustas, W.P.** 2008: Thermal remote sensing of drought and evaporation. *EOS* 89(26), 233–40.
- Anderson, M.C., Norman, J.M., Kustas, W.P., Houborg, R., Starks, P.J. and Agam, N.** 2008: A thermal-based remote sensing technique for routine mapping of land-surface carbon, water and energy fluxes from field to regional scales. *Remote Sensing of Environment* 112, 4227–41.
- André, J.-C., Goutorbe, J.-P. and Perrier, A.** 1986: HAPEX–Mobilhy: a hydrologic atmospheric experiment for the study of water budget and evaporation flux at the climatic scale. *Bulletin of the Americal Meteorological Society* 67, 138–44.
- Arthur, T., Hartanft, S.T., Carlson, T.N. and Clarke, K.C.** 2003: Satellite and ground-based microclimate and hydrologic analyses coupled with a regional urban growth model. *Remote Sensing of Environment* 86, 385–400.
- Bastiaanssen, W.G.M.** 1995: Regionalization of surface flux densities and moisture indicators in composite terrain. PhD thesis, Wageningen, Agricultural University (appeared also as Report 109, DLO-Winand Staring centre), Wageningen, The Netherlands, 273 pp.
- Bastiaanssen, W., Menenti, M., Feddes, R., and Holtslag, A.** 1998: A remote sensing surface energy balance algorithm for land (SEBAL). 1. Formulation. *Journal of Hydrology* 212–213, 198–212.
- Batra, N., Islam, S., Venturini, V., Bisht, G. and Jiang, L.** 2006: Estimation and comparison of evapotranspiration from MODIS and AVHRR for clear sky days over the Southern Great Plains. *Remote Sensing of Environment* 103, 1–15.
- Brunsell, N.A. and Gillies, R.R.** 2003: Scale issues in land-atmosphere interactions: implications for remote sensing of the surface energy balance. *Agricultural and Forest Meteorology* 117, 203–21.
- Calvet, J.C. and Noilhan, J.** 2000: From near-surface to root-zone soil moisture using year-round data. *Journal of Hydrometeorology* 1, 393–411.
- Caparrini, F., Castelli, F. and Entekhabi, D.** 2003: Mapping of land atmosphere heat fluxes and surface parameters with remote sensing data. *Boundary layer Meteorology* 107, 605–33.
- Capehart, W.J. and Carlson, T.N.** 1994: Estimating near surface soil moisture availability using meteorologically-driven soil water profile model. *Journal of Hydrology* 160, 1–20.
- 1997: Decoupling of surface and near-surface soil water content: a remote sensing perspective. *Water Resources Research* 33, 1383–95.
- Carlson, T.N.** 2007: An overview of the 'triangle method' for estimating surface evapotranspiration and soil moisture from satellite imagery. *Sensors* 7, 1612–29.
- Carlson, T.N. and Arthur, S.T.** 2000: The impact of land use – land cover changes due to urbanization on surface microclimate and hydrology: a satellite perspective. *Global and Planetary Change* 25, 49–65.
- Carlson, T.N. and Buffum, M.J.** 1989: On estimating the total daily evapotranspiration from remote surface temperature measurements. *Remote Sensing Environment* 29, 197–207.
- Carlson, T.N. and Ripley, D.A.** 1997: On the relation between NDVI, fractional vegetation cover, and leaf area index. *Remote Sensing of Environment* 62, 241–52.
- Carlson, T.N. and Sanchez-Azofeifa, G.A.** 1999: Satellite remote sensing of land use changes in and around San José, Costa Rica. *Remote Sensing of Environment* 70, 247–56.
- Carlson, T.N., Capehart, W.J. and Gillies, R.R.** 1995a: A new look at the simplified method for remote sensing of daily evapotranspiration. *Remote Sensing of Environment* 54, 161–67.
- Carlson, T.N., Dodd, J.K., Benjamin, S.G. and Cooper, J.N.** 1981: Satellite estimation of the surface energy balance, moisture availability and thermal inertia. *Journal of Applied Meteorology* 20, 67–87.
- Carlson, T.N., Gillies, R.R. and Schmugge, T.J.** 1995b: An interpretation of methodologies for indirect measurement of soil water content. *Agricultural and Forest Meteorology* 77, 191–205.
- Carlson, T.N., Perry, E.M. and Schmugge, T.J.** 1990: Remote estimation of soil moisture availability and fractional vegetation cover for agricultural fields. *Agricultural and Forest Meteorology* 52, 45–69.
- Chauhan, N.S., Miller, S. and Ardanuy, P.** 2003: Spaceborne soil moisture estimation at high resolution: a microwave-optical/IR synergistic approach. *International Journal of Remote Sensing* 24, 4599–622.

- Chen, J.-H., Kan, C.-E., Tan, C.-H. and Shih, S.-F.** 2002: Use of spectral information for wetland evapotranspiration assessment. *Agricultural Water Management* 55, 239–48.
- Choudhury, B.J., Ahmed, N.U., Idso, S.B., Reginato, R.J. and Daughtry, C.S.T.** 1994: Relations between evaporation coefficients and vegetation indices studied by model simulations. *Remote Sensing of Environment* 50, 1–17.
- Consoli, S., Urso, G. and Toscano, A.** 2006: Remote sensing to estimate ET-fluxes and the performance of an irrigation district in southern Italy. *Agricultural Water Management* 81, 295–314.
- Courault, D., Seguin, B. and Olioso, A.** 2005: Review on estimation of evapotranspiration from remote sensing data: from empirical to numerical modelling approaches. *Irrigation and Drainage Systems* 19, 223–49.
- Crombie, M.K., Gillies, R.R., Arvidson, R.E., Brookmeyer, P., Weil, G.J., Sultan, M. and Harb, M.** 1999: An application of remotely-derived climatological fields for risk assessment of vector-borne diseases – a spatial study of filariasis prevalence in the Nile Delta, Egypt. *Photogrammetric Engineering and Remote Sensing* 65, 1401–409.
- de Troch, F.P., Troch, P.A., Su, Z. and Lin, D.S.** 1996: Application of remote sensing for hydrological modelling. In Abbott, M.B. and Refsgaard, J.C., editors, *Distributed hydrological modelling*, Dordrecht: Kluwer, 165–91.
- Dodds, P.E., Meyer, W.S. and Barton, A.** 2005: A review of methods to estimate irrigated reference crop evapotranspiration across Australia. Document prepared for Irrigation Features Technical Report, Australia. Retrieved 15 May 2009 from <http://www.clw.csiro.au/publications/consultancy/2005/CRCIFtr04-05-CropEvapotranspiration.pdf#search=%22A%20review%20of%20methods%20to%20estimate%20irrigated%20reference%20crop%20evapotranspiration%20across%20Australia.%20%22>
- Engman, E.T. and Schultz, G.A.** 2000: Future perspectives. In Schultz, G.A. and Engman, E.T., editors, *Remote sensing in hydrology and water management*, Berlin: Springer, 445–57.
- Gillies, R.R. and Carlson, T.N.** 1995: Thermal remote sensing of surface soil water content with partial vegetation cover for incorporation into climate models. *Journal of Applied Meteorology* 34, 745–56.
- Gillies, R.R. and Temesgen, B.** 2000: Coupling thermal infrared and visible satellite measurements to infer biophysical variables at the land surface. In Quattrochi, D.A. and Luvall, J.C., editors, *Thermal remote sensing in land surface processes*, New York: CRC Press, 160–83.
- Gillies, R.R., Carlson, T.N., Cui, J. Kustas, W.P. and Humes, K.S.** 1997: Verification of the ‘triangle’ method for obtaining surface soil water content and energy fluxes from remote measurements of the Normalized Difference Vegetation Index NDVI and surface radiant temperature. *International Journal of Remote Sensing* 18, 3145–66.
- Goetz, S.J.** 1997: Multi-sensor analysis of NDVI, surface temperature and biophysical variables at a mixed grassland site. *International Journal of Remote Sensing* 18, 71–94.
- Gomez, M., Olioso, A., Sobrino, J.A. and Jacob, F.** 2005: Retrieval of evapotranspiration over the Aplilles/ReSeDA experimental site using airborne POLDER sensor and a thermal camera. *Remote Sensing of Environment* 96, 399–408.
- Goward, S.N., Cruickhanks, G.D. and Hope, A.S.** 1985: Observed relation between thermal emission and reflected spectral radiance of a complex vegetated landscape. *Remote Sensing of Environment* 18, 137–46.
- Goward, S.N., Xue, Y. and Czajkowski, K.P.** 2002: Evaluating land surface moisture conditions from the remotely sensed temperature/vegetation index measurements: an exploration with the simplified simple biosphere model. *Remote Sensing of Environment* 79, 225–42.
- Hope, A.S., Petzold, D.E., Goward, S.N. and Ragan, R.M.** 1986: Simulated relationships between spectral reflectance, thermal emissions and evapotranspiration of a soybean canopy. *Water Resources Bulletin* 22, 1011–19.
- Jackson, R.D., Idso, D.B., Reginato, R.J. and Pinter, P.J.** 1981: Canopy temperature as a crop water stress indicator. *Water Resources Research* 17, 1133–38.
- Jacob, F., Olioso, A., Su, Z. and Seguin, B.** 2002: Mapping surface fluxes using airborne visible, near infrared, thermal infrared remote sensing data and a spatialized surface energy balance model. *Agronomie* 22, 669–80.
- Jiang, L. and Islam, S.** 1999: A methodology for estimation of surface evapotranspiration over large areas using remote sensing observations. *Geophysical Research Letters* 26, 2773–76.
- 2001: Estimation of surface evaporation map over Southern Great Plains using remote sensing data. *Water Resources Research* 37, 329–40.
- 2003: An intercomparison of regional heat flux estimation using remote sensing data. *International Journal of Remote Sensing* 24, 2221–36.
- Jiang, L., Islam, S. and Carlson, T.N.** 2004: Uncertainties in latent heat flux measurement and estimation: implications for using a simplified approach with remote sensing data. *Canadian Journal of Remote Sensing* 30, 769–87.
- Jordan, J.D. and Shih, S.F.** 2000: Satellite-based diurnal and seasonal thermal patterns of natural, agricultural, and urban land-cover vs. soil type



- in Florida. In *Proceedings of the 2nd International Conference on Geospatial Information in Agriculture and Forestry (ICGIAF)*, volume 1, 10–12 January, Lake Buena Vista, Florida, 489–95.
- Kustas, W.P., Goodrich, D.C., Moran, M.S., Amer, S.A., Bach, L.B., Blanford, J.H., Chehbouni, A., Claasen, H., Clements, W.E., Doraiswamy, P.C., Dubois, P., Huete, A.R., Humes, K.S., Jackson, T.J., Kiefer, T.O., Nichols, W.D., Parry, R., Perry, E.M., Pinker, R., Pinter, J., Schmugge, T.J., Stannard, D.I., Vidal, A., Washburne, J. and Weltz, M.A.** 1991: An interdisciplinary field study of the energy and water fluxes in the atmosphere-biosphere system over semi-arid rangelands: description and some preliminary results. *Bulletin of the American Meteorological Society*, 72, 1683–705.
- Kustas, W.P., Jackson, T.J., Prueger, J.H., MacPherson, J.I. and Wolde, M.** 2004: Effects of remote sensing pixel resolution on modelled energy flux variability of croplands in Iowa. *Remote Sensing of Environment* 92, 535–47.
- Lambin, E.F. and Ehrlich, D.** 1996: The surface temperature-vegetation index space for land cover and land cover-change analysis. *International Journal of Remote Sensing* 17, 463–87.
- Li, F. and Lyons, T.J.** 1998: Estimation of regional evapotranspiration through remote sensing. *Journal of Applied Meteorology* 38, 1644–54.
- Li, F., Kustas, W.P., Anderson, M.C., Prueger, J.H. and Scott, R.** 2008: Effect of remote sensing spatial resolution on interpreting tower-based flux observations. *Remote Sensing of Environment* 112, 337–49.
- Lyons, T.J., Schwerdtfeger, P., Hacker, J.M., Foster, I.J., Smith, R.C.G. and Huang, X.** 1993: Land-atmosphere interaction in a semiarid region: the bunny fence experiment. *Bulletin of the American Meteorological Society* 74, 1327–34.
- Mallick, K., Bhattacharya, B.K. and Patel, N.K.** 2009: Estimating volumetric surface moisture content for cropped soils using a soil wetness index based on surface temperature and NDVI. *Agricultural and Forest Meteorology*, in press.
- Margulis, S., Kim, J. and Hogue, T.** 2005: A comparison of the triangle retrieval and variational data assimilation methods for surface turbulent flux estimation. *Journal of Hydrometeorology* 6, 1063–72.
- McCabe, M.F. and Wood, E.F.** 2006: Scale influences on the remote estimation of evapotranspiration using multiple satellite sensors. *Remote Sensing of Environment* 105, 271–85.
- Menenti, M., Bastiaanssen, W.G.M., van Eick, D. and Abd El Karim, M.H.** 1989: Linear relationships between surface reflectance and temperature and their application to map evaporation of groundwater. *Advances in Space Research* 9, 165–76.
- Moran, M.S., Clarke, T.R., Inoue, Y. and Vidal, A.** 1994: Estimating crop water deficit using the relation between surface-air temperature and spectral vegetation index. *Remote Sensing of Environment* 49, 246–63.
- Moran, M.S., Peters-Lidard, C.D., Watts, J.M. and McElroy, S.** 2004: Estimating soil moisture at the watershed scale with satellite-based radar and land surface models. *Canadian Journal of Remote Sensing* 30, 805–24.
- Moran, M.S., Rahman, A.F., Washburne, J.C., Goodrich, D.C., Weltz, M.A. and Kustas, W.P.** 1996: Combining the Penman-Monteith equation with measurements of surface temperature and reflectance to estimate evaporation rates of semi-arid grassland. *Agricultural and Forest Meteorology* 80, 87–109.
- Mu, Q., Heinsch, F.A., Zhao, M. and Running, S.** 2007: Development of a global evapotranspiration algorithm based on MODIS and global meteorology data. *Remote Sensing of Environment* 111, 519–36.
- Murray, T. and Verhoef, A.** 2007: Moving towards a more mechanistic approach in the determination of soil heat flux from remote measurements. I. A universal approach to calculate thermal inertia. *Agricultural and Forest Meteorology* 147, 80–87.
- Nemani, R.R. and Running, S.** 1989: Estimation of regional surface resistance to evapotranspiration from NDVI and thermal IR AVHRR data. *Journal of Applied Meteorology* 28, 276–84.
- Nemani, R.R., Pierce, L., Running, S. and Goward, S.** 1993: Estimation of regional surface resistance to evapotranspiration from NDVI and thermal-IR AVHRR data. *Journal of Applied Meteorology* 32, 548–57.
- Nishida, K., Nemani, R.R., Glassy, J. and Running, S.W.** 2003a: Development of an evapotranspiration index from Aqua/MODIS for monitoring surface moisture status. *IEEE Transactions on Geoscience and Remote Sensing* 41, 493–501.
- Nishida, K., Nemani, R.R., Running, S.W. and Glassy, J.M.** 2003b: An operational remote sensing algorithm of land surface evaporation. *Journal of Geophysical Research* 108(D9), 4270, DOI: 10.1029/2002JD002062.
- Noilhan, J. and Planton, S.** 1989: A simple parameterization of land surface processes for meteorological models. *Monthly Weather Review* 117, 536–49.
- Norman, J., Kustas, W. and Humes, K.** 1995: A two-source approach for estimating soil and vegetation energy fluxes from observations of directional radiometric surface temperature. *Agricultural and Forest Meteorology* 77, 263–93.
- Owen, T.W., Carlson, T.N. and Gillies, R.R.** 1998: Remotely sensed surface parameters governing urban climate change. *International Journal of Remote Sensing* 19, 1663–81.

- Parida, B.R.** 2006: Analyzing the effect of severity and duration of agricultural drought on crop performance using Terra/MODIS satellite data and meteorological data. MSc dissertation, Institute for Geoinformation Science and Earth Observation, Netherlands, 86 pp. Available online from ITC library.
- Price, J.C.** 1990: Using spatial context in satellite data to infer regional scale evapotranspiration. *IEEE Transactions on Geoscience and Remote Sensing* 28, 940–48.
- Prihodko, L.** and **Goward, S.N.** 1997: Estimation of air temperature from remotely sensed surface observations. *Remote Sensing of Environment* 60, 335–46.
- Ridd, M.** 1995: Exploring a V-I-S (vegetation-impervious surface-soil) model for urban ecosystem analysis through remote sensing: comparative anatomy of cities. *International Journal of Remote Sensing* 16, 2165–85.
- Roerink, G.J., Su, Z.** and **Menenti, M.** 2000: S-SEBI: A simple remote sensing algorithm to estimate the surface energy balance. *Physics and Chemistry of the Earth, part B: Hydrology, Oceans and Atmosphere* 25, 147–57.
- Sanchez, J.M., Kustas, W.P., Caselles, V.** and **Anderson, M.C.** 2008: Modelling surface energy fluxes over maize using a two-source patch model and radiometric soil and canopy temperature observations. *Remote Sensing of Environment* 112, 1130–43.
- Sandholt, I., Rasmussen, K.** and **Andersen, J.** 2002: A simple interpretation of the surface temperature/vegetation index space for assessment of soil moisture status. *Remote Sensing of Environment* 79, 213–24.
- Seguin, B., Becker, F., Phulpin, T., Gu, X.F., Guyot, G., Kerr, Y., King, C., Lagouarde, J.P., Ottlé, C., Stoll, M.P., Tabbagh, A.** and **Vidal, A.** 1999: IRSUTE: A minisatellite project for land surface heat flux estimation from field to regional scale. *Remote Sensing of Environment* 68, 357–69.
- Sellers, P.J., Hall, F.G., Asrar, G., Strubel, D.E.** and **Murthy, R.E.** 1992: An overview of the First International Satellite Land Surface Climatology project (ISLSCP) Field Experiment (FIFE). *Journal of Geophysical Research* 97, 18345–71.
- Shuttleworth, W.J., Gurney, R.J., Hsu, A.Y.** and **Ormsby, J.P.** 1989: FIFE: the variation in energy partition at surface flux sites. *IAHS Publication* 186, 67–74.
- Smith, R.C.G.** and **Choudhury, B.J.** 1991: Analysis of normalized difference and surface temperature observations over southeastern Australia. *International Journal of Remote Sensing* 12, 2021–44.
- Sobrino, J.A., Gómez, M., Jiménez-Muñoz, J.C.** and **Olioso, A.** 2007: Application of a simple algorithm to estimate daily evapotranspiration from NOAA-AVHRR images for the Iberian Peninsula. *Remote Sensing of Environment* 110, 139–48.
- Sobrino, J.A., Gomez, M., Jimenez-Munoz, J., Olioso, A.** and **Chehbouni, G.** 2005: A simple algorithm to estimate evapotranspiration from DAIS data: application to the DAISEX campaigns. *Journal of Hydrology* 315, 117–25.
- Stisen, S., Sandholt, I., Norgaard, A., Fensholt, R.** and **Eklundh, L.** 2007: Estimation of diurnal air temperature using MSG SEVIRI data in West Africa. *Remote Sensing of Environment* 110, 262–74.
- Stisen, S., Sandholt, I., Norgaard, A., Fensholt, R.** and **Jensen, K.H.** 2008: Combining the triangle method with thermal inertia to estimate regional evapotranspiration – applied to MSG SEVIRI data in the Senegal River basin. *Remote Sensing of Environment* 112, 1242–55.
- Su, Z.** 2002: The surface energy balance system (SEBS) for estimation of the turbulent heat fluxes. *Hydrology and Earth Sciences* 6, 85–99.
- Sun, Y.-J., Wang, J.-F., Zhang, R.-H., Gillies, R.R., Xue, Y.** and **Bo, Y.-C.** 2005: Air temperature retrieval from remote sensing data based on thermodynamics. *Theoretical and Applied Climatology* 80, 37–48.
- Symanzik, J., Griffiths, L.** and **Gillies, R.** 2000: Visual exploration of satellite images. In *Proceedings of the Statistical Computing Section and Section on Statistical Graphics*, Alexandria, VA: American Statistical Association, 10–19.
- Tan, C.-H.** 1998: Regional scale evapotranspiration estimation using vegetation index and surface temperature from NOAA AVHRR satellite data. PhD thesis, University of Florida, 244 pp.
- van de Griend, A.A., Camillo, P.J.** and **Gurney, R.J.** 1985: Discrimination of soil physical parameters, thermal inertia, and soil moisture from diurnal surface temperature fluctuations. *Water Resources Research* 21, 997–1009.
- Venturini, V., Bisht, G., Islam, S.** and **Jiang, L.** 2004: Comparison of evaporative fractions estimated from AVHRR and MODIS sensors over South Florida. *Remote Sensing of Environment* 93, 77–86.
- Verstraeten, W.W., Veroustraete, F.** and **Feyen, J.** 2008: Assessment of evapotranspiration and soil moisture content across different scales of observation. *Sensors* 8, 70–117.
- Wan, Z., Wang, P.** and **Li, X.** 2004: Using MODIS land surface temperature and Normalized Difference Vegetation Index products for monitoring drought in the Southern Great Plains, USA. *International Journal of Remote Sensing* 25, 61–72.
- Wang, K., Li, Z.** and **Cribb, M.** 2006: Estimation of evaporative fraction from a combination of day and night land surface temperatures and NDVI: a new method to determine the Priestley-Taylor parameter. *Remote Sensing of Environment* 102, 293–305.
- Wever, L., Flanagan, L.** and **Carlson, P.J.** 2002: Seasonal and interannual variation in evapotranspiration, energy balance and surface conductance

in a northern temperate grassland. *Agricultural and Forest Meteorology* 112, 31–49.

**Xu, C.Y.** and **Chen, D.** 2005: Comparison of seven models for estimation of evapotranspiration and groundwater recharge using lysimeter measurement data in Germany. *Hydrological Processes* 19, 3717–34.

**Yepez, E.A., Williams, D.G., Scott, R.L.** and **Lin, G.** 2003: Partitioning overstorey and understorey evapotranspiration in a semiarid savanna woodland from the isotopic composition of water vapour. *Agricultural and Forest Meteorology* 119, 53–68.